Supporting Information:

Crowding Effects on Energy Transfer Efficiencies of Hetero-FRET Probes as Measured using Time-Resolved Fluorescence Anisotropy

Hannah Leopold [†], Ryan Leighton[†], Jacob Schwarz [†], Arnold J. Boersma[‡], Erin D. Sheets[†*] and Ahmed A. Heikal[†*]

[†] *Department of Chemistry and Biochemistry, Swenson College of Science and Engineering, University of Minnesota Duluth, Duluth, MN, USA*

[‡]*DW1-Leibniz Institute for Interactive Materials, Forckenbeckstr.50, 52056 Aachen, Germany.*

***** Corresponding Authors: *Ahmed A. Heikal (aaheikal@d.umn.edu, 218-726-7036); Erin D. Sheets* (edsheets@d.umn.edu*, 218-726-6046*).

Supporting Information: Figures

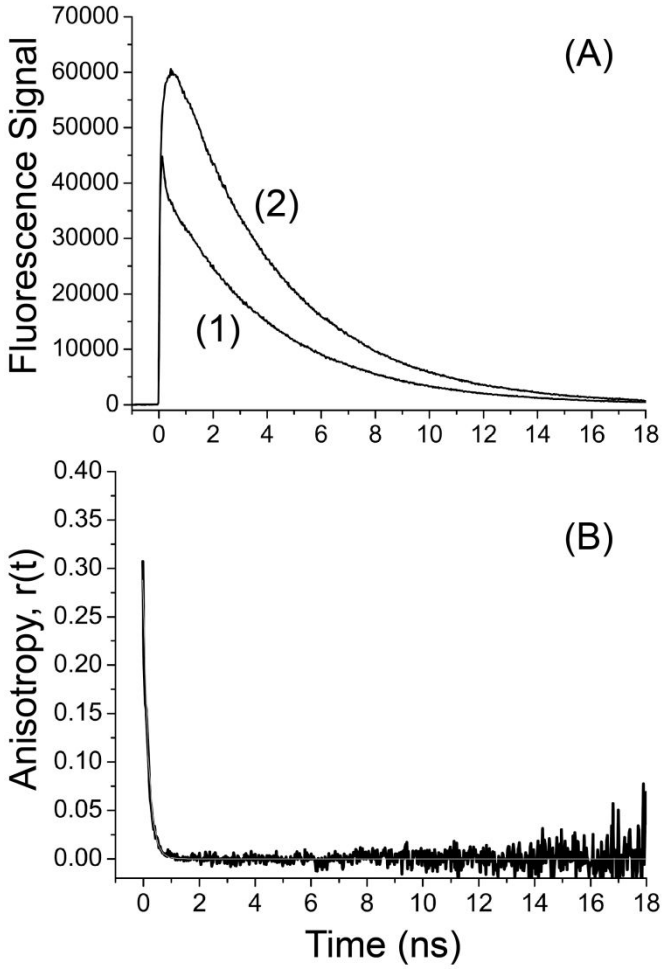

Figure S1: Time-resolved fluorescence anisotropy of rhodamine-110 for calibrating the G-factor in our experimental setup. (A) Time-resolved parallel (curve 1) and perpendicular (curve 2) fluorescence of Rh110 (PBS, pH 7.5) were detected simultaneously using SPC-830 module. Rh110 was excited at 425 nm with polarization-analyzed fluorescence that was detected at 531/40 nm. Notice the high signal to noise ratio required for reliable time-resolved anisotropy calculations, particularly for large molecules with a rotational time that significantly longer than the excited-state lifetime (4.0 ns for Rh110). (B) Time-resolved anisotropy of Rh110 (PBS, pH 7.5) reveals a rotational time of 180 ps due to the ester group attached to this reference fluorophore. Our estimated a G-factor of 0.556 using tail-matching approach of the parallel and perpendicular fluorescence decays (Panel A). This control experiment was carried out multiple times during measurements of time-resolved anisotropy of the other hetero-FRET probes.

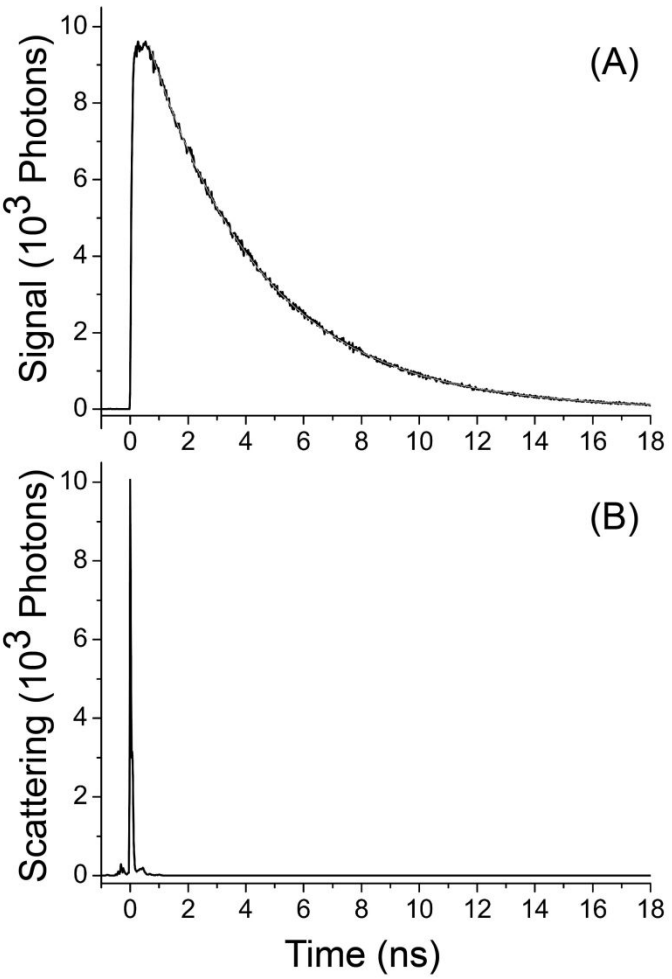

Figure S2: Excited-state fluorescence lifetime measurements of the donor in cleaved E6 (PBS, pH 7.5). (A) Time-resolved fluorescence of cleaved E6 (PBS, pH 7.5), which was excited at 425 nm with magic-angle detection at 475/50 nm. The fluorescence decay is shown on a logarithmic scale along with the fitting curve (gray) with an estimated average fluorescence lifetime of 3.97 ± 0.04 ns. (B) The measured system response function (SRF) of our setup has a full width half maximum (FWHM) of 60 ps. The SRF was measured by detecting the scattered light of the laser on a droplet of 2% milk replacing our fluorescent sample. The emission filters were removed from the detection system during the SRF measurements under the same SPC-830 setup and in the presence of the dichroic mirror.

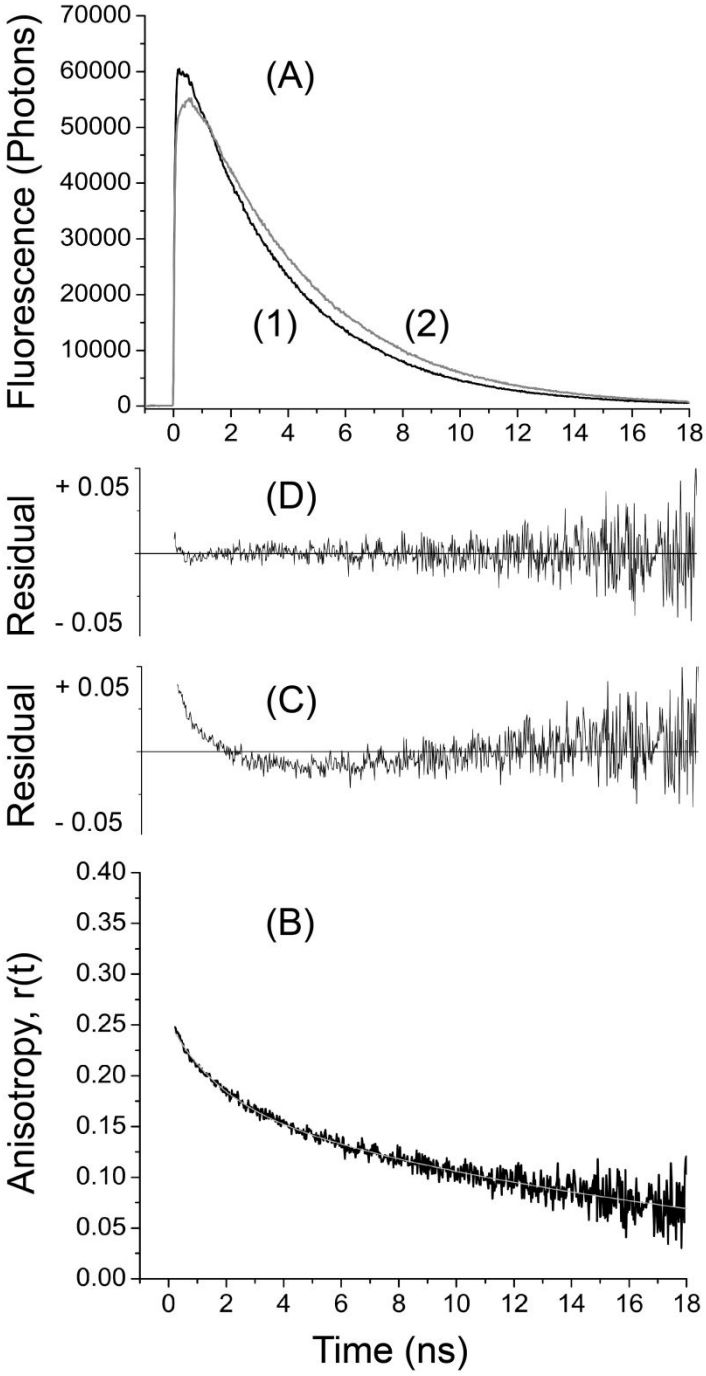

Figure S.3: Time-resolved fluorescence anisotropy of intact E6 FRET probe. (A) Typical time-resolved fluorescence of parallel (curve 1) and perpendicular (curve 2) polarizations of intact E6 (PBS, pH 7.5), where the donor was excited at 425 nm and the emission of the acceptor was detected at 531/40 nm. (B) The corresponding time-resolved anisotropy of intact E6 as calculated from (A). (C) The residual of a single-exponential fitting model of the time-resolved anisotropy of intact E6 (PBS) is modulated suggesting inadequate description of the rotational dynamics of E6 under these excitation and detection conditions. (D) The residual of a double exponential fitting model of the time-resolved anisotropy of intact E6 (PBS), with the fitting parameters are $\beta_1 = 0.08$, $\varphi_1 = 1.73$ ns, $\beta_2 = 0.18$, and $\varphi_2 = 19.0$ ns. The G-factor was measured daily using Rh110 (Figure S.2) under the same experimental conditions for reliable calibration of our setup during the time-resolved anisotropy measurements of all other hetero-FRET probes.

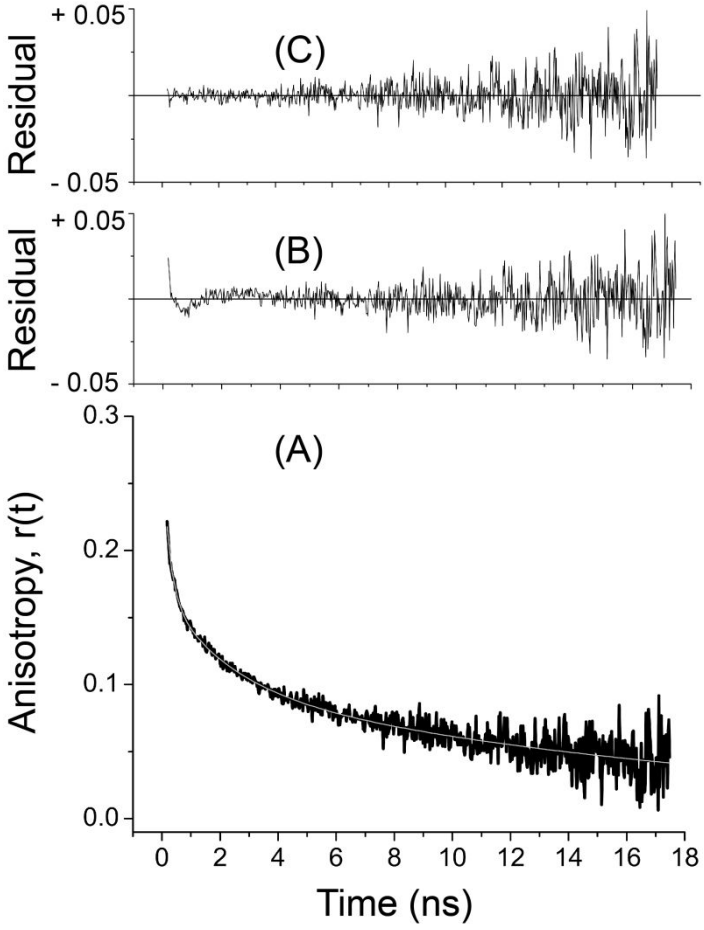

Figure S4: Time-resolved fluorescence anisotropy of intact G12 FRET probe. (A) Typical time-resolved anisotropy of intact G12 (PBS, pH 7.5), where the donor was excited at 425 nm and the emission of the acceptor was detected at 531/40 nm. (B) The residual of a double-exponential fitting model of the time-resolved anisotropy of intact G12 (PBS) is modulated suggesting inadequate description of the rotational dynamics of G12 under these excitation and detection conditions. (C) The corresponding residual of a triple-exponential fitting model of the time-resolved anisotropy of intact G12 (PBS) with β_1= 0.11, φ_1= 0.25 ns, β_2 = 0.07, φ_2 = 2.19 ns, β_3 = 0.10, and φ_3 = 19.8 ns. Similar trend was observed for G18 FRET probe with β_1= 0.08, φ_1 = 0.24 ns, β_2 = 0.07, φ_2 = 1.94 ns, β_3 = 0.12, and φ_3 = 18.1 ns, under the same experimental conditions.

Supporting Information: Tables

Table S1: Fitting parameters of the wavelength-dependent time-resolved fluorescence anisotropy of intact and cleaved E6 probe (PBS, pH 7.4). The angle (θ) between the absorbing and emitting dipoles is also calculated using the initial anisotropy (r_0).

$\lambda_x - \lambda_{fl}$: Probe	β_1	φ_1 (ns)	β_2	φ_2 (ns)	r_0	θ
425 – 475/50:						
Intact E6	—	—	0.280	17.8	0.280	46.6°
Cleaved E6	—	—	0.287	13.3	0.287	46.3°
425 – 531/40:						
Intact E6	0.074	1.47	0.184	18.0	0.258	47.8°
Cleaved E6	—	—	0.283	14.1	0.283	46.5
465 – 531/40:						
Intact E6	0.058	1.95	0.197	19.3	0.255	47.9°
Cleaved E6	—	—	0.280	14.9	0.280	46.6°

Table (S2): Fitting parameters of the E6 FRET probe (excited at 425 nm and detected at 531/40 nm) in Ficoll-70 and glycerol solutions (in PBS). The calculated energy transfer rates (k_{ET}), the apparent energy transfer efficiencies (E), and the donor-acceptor distances (R_{DA}) are also shown.

Environment (PBS)	β_1	φ_1 (ns)	β_2	φ_2 (ns)	τ_D (ns)	k_{ET} (ns^{-1})	E^a (%)	R_{DA} (nm)
Ficoll:								
0 g/L	0.074	1.47	0.184	17.96	3.98	0.625	20.5	6.60
100 g/L	0.078	1.57	0.159	26.49	3.91	0.599	23.1	6.40
200 g/L	0.085	1.51	0.144	49.61	3.81	0.642	26.3	6.19
300 g/L	0.086	1.12	0.142	78.22	3.74	0.880	28.9	5.97
Glycerol:								
0 g/L	0.074	1.47	0.184	17.96	3.98	0.625	20.5	6.60
340 g/L	0.068	1.32	0.2	35.01	3.73	0.729	18.6	6.64
480 g/L	0.072	1.9	0.2	64.46	3.61	0.511	17.2	6.68
620 g/L	0.075	1.74	0.205	91.12	3.50	0.564	17.8	6.57
760 g/L	0.075	2.23	0.202	183.24	3.34	0.443	16.2	6.66

Table (S3): Fitting parameters of the GE FRET probe (excited at 425 nm and detected at 531/40 nm) in Ficoll-70 and glycerol solutions (in PBS). The calculated energy transfer rate, the apparent energy transfer efficiencies, and the donor-acceptor distance are also shown.

Environment (PBS)	β_1	φ_1 (ns)	β_2	φ_2 (ns)	τ_D (ns)	k_{ET} (ns^{-1})	E^a (%)	R_{DA} (nm)
Ficoll:								
0 g/L	0.055	1.7	0.212	18.06	3.99	0.533	14.0	7.12
100 g/L	0.064	1.68	0.189	27.78	3.89	0.559	17.3	6.79
200 g/L	0.069	1.38	0.18	51.29	3.82	0.705	20.2	6.55
300 g/L	0.069	1.43	0.177	101.05	3.75	0.689	20.2	6.46
Glycerol:								
0 g/L	0.055	1.7	0.212	18.06	3.99	0.533	14.0	7.12
340 g/L	0.051	2.28	0.222	44.72	3.74	0.416	11.4	7.30
480 g/L	0.050	2.23	0.231	74.54	3.63	0.435	10.9	7.29
620 g/L	0.047	2.08	0.236	100.36	3.52	0.471	10.4	7.29
760 g/L	0.045	2.42	0.243	150.67	3.35	0.407	9.0	7.44

Table (S4): Fitting parameters of the G18 FRET probe (excited at 425 nm and detected at 531/40 nm) in Ficoll-70 and glycerol solutions (in PBS). The calculated energy transfer rates, the apparent energy transfer efficiencies, and the donor-acceptor distances are also shown.

Environment (PBS)	β_1	φ_1 (ns)	β_2	φ_2 (ns)	τ_D (ns)	k_{ET} (ns^{-1})	E^a (%)	R_{DA} (nm)
Ficoll:								
0 g/L	0.092	1.06	0.129	16.2	3.97	0.882	32.4	5.95
100 g/L	0.096	1.21	0.105	32.21	3.89	0.795	36.1	5.76
200 g/L	0.095	1.14	0.104	65.47	3.79	0.862	36.5	5.71
300 g/L	0.100	1.18	0.097	∞	3.72	0.847	38.5	5.55
Glycerol:								
0 g/L	0.092	1.06	0.129	16.2	3.97	0.882	32.4	5.95
340 g/L	0.095	1.36	0.133	42	3.71	0.711	30.2	5.96
480 g/L	0.102	1.24	0.131	84.96	3.59	0.795	32.4	5.81
620 g/L	0.103	1.35	0.136	136.25	3.44	0.733	30.9	5.82
760 g/L	0.101	1.47	0.145	218.96	3.30	0.676	28.3	5.91

Table (S5): Fitting parameters of the E6G2 FRET probe (excited at 425 nm and detected at 531/40 nm) in Ficoll-70 and glycerol solutions (in PBS). The calculated energy transfer rates, the apparent energy transfer efficiencies, and the donor-acceptor distances are also shown.

Environment (PBS)	β_1	φ_1 (ns)	β_2	φ_2 (ns)	τ_D (ns)	k_{ET} (ns^{-1})	E^a (%)	R_{DA} (nm)
Ficoll:								
0 g/L	0.068	1.28	0.194	18.83	3.99	0.728	19.3	6.68
100 g/L	0.073	1.39	0.181	26.88	3.91	0.682	20.9	6.54
200 g/L	0.079	1.2	0.162	47.65	3.83	0.812	24.8	6.27
300 g/L	0.084	1.04	0.149	120.01	3.75	0.953	28.2	6.00
Glycerol:								
0 g/L	0.068	1.28	0.194	18.83	3.99	0.728	19.3	6.68
340 g/L	0.065	1.52	0.212	45.81	3.73	0.636	16.5	6.79
480 g/L	0.066	1.57	0.213	79.73	3.61	0.624	16.4	6.74
620 g/L	0.064	1.5	0.22	108.23	3.475	0.657	15.7	6.73
760 g/L	0.065	1.88	0.227	159.21	3.31	0.526	14.1	6.84

Table (S6): Fitting parameters of the G12 FRET probe (excited at 425 nm and detected at 531/40 nm) in Ficoll-70 and glycerol solutions (in PBS). The calculated energy transfer rates, the apparent energy transfer efficiencies, and the donor-acceptor distances are also shown.

Environment (PBS)	β_1	φ_1 (ns)	β_2	φ_2 (ns)	τ_D (ns)	k_{ET} (ns^{-1})	E^a (%)	R_{DA} (nm)
Ficoll:								
0 g/L	0.099	1.06	0.114	16.57	3.98	0.883	36.2	5.78
100 g/L	0.101	1.17	0.104	28.15	3.88	0.819	37.5	5.70
200 g/L	0.101	1.11	0.097	47.04	3.81	0.880	39.3	5.60
300 g/L	0.103	1.02	0.093	235.1	3.74	0.976	41.3	5.45
Glycerol:								
0 g/L	0.099	1.06	0.114	16.57	3.98	0.883	36.2	5.78
340 g/L	0.105	1.36	0.121	44.35	3.71	0.713	33.7	5.80
480 g/L	0.105	1.36	0.128	63.24	3.58	0.719	32.5	5.80
620 g/L	0.105	1.48	0.133	90.65	3.44	0.665	30.7	5.83
760 g/L	0.107	1.93	0.142	185.01	3.28	0.513	26.9	5.98

Table (S7): A summary of the energy-transfer efficiencies of the five hetero-FRET probes in Ficoll-70 and glycerol solutions (in PBS). The Forster distances used in the energy transfer efficiency calculations are also shown, which were calculated based on the steady-state spectroscopy in different environments.

Environment (PBS)	**GE**	**G18**	**E6**	**E6G2**	**G12**	**R_0** (nm)
Ficoll:						
0 g/L	14.0	32.4	20.5	19.3	36.2	5.26
100 g/L	17.3	36.1	23.1	20.9	37.5	5.24
200 g/L	20.2	36.6	26.4	24.8	39.3	5.21
300 g/L	20.2	38.5	28.9	28.2	41.3	5.14
Glycerol:						
0 g/L	14.0	32.4	20.5	19.3	36.2	5.26
340 g/L	11.4	30.2	18.6	16.5	33.7	5.19
480 g/L	10.9	32.4	17.2	16.4	32.5	5.14
620 g/L	10.4	30.9	17.8	15.7	30.7	5.09
760 g/L	9.0	28.4	16.2	14.1	26.9	5.06

Table S8: Fitting parameters of the time-resolved anisotropy for all constructs in PBS (pH 7.4) under 425 nm excitation and 531/40 nm detection. The angle (θ) between the absorbing and emitting dipoles is also calculated using the initial anisotropy. The corresponding apparent energy transfer efficiencies (E) and donor-acceptor distances (R_{DA}) are also shown.

$\lambda_x - \lambda_{fl}$: Probe	β_1	φ_1 (ns)	β_2	φ_2 (ns)	r_0	θ	E	R_{DA} (nm)
425 – 531/40:								
GE	0.055	1.70	0.212	18.1	0.267	47.3°	14.0%	7.12
E6G2	0.068	1.28	0.194	18.8	0.262	47.6°	19.3%	6.68
E6	0.074	1.47	0.184	18.0	0.258	47.8°	20.5%	6.60
G18	0.092	1.06	0.129	16.2	0.221	49.7°	32.4%	5.95
G12	0.099	1.06	0.114	16.6	0.213	50.1°	36.2%	5.78

Table S9: Fitting parameters of time-resolved anisotropy of representative intact and cleaved E6 proteins in glycerol-enriched buffer at room temperature. The angle (θ) between the absorbing and emitting dipoles is also calculated using the initial anisotropy. The corresponding donor-acceptor distances (R_{DA}) is also shown based on the apparent energy transfer efficiencies.

$\lambda_x - \lambda_{fl}$:	β_1	φ_1	β_2	φ_2	r_0	R_{DA}
425 – 531/40:		**(ns)**		**(ns)**		**(nm)**
E6						
340 g/L	0.068	1.32	0.200	35.0	0.269	6.64
480 g/L	0.072	1.90	0.200	64.5	0.272	6.68
620 g/L	0.075	1.74	0.205	91.1	0.269	6.57
760 g/L	0.075	2.23	0.202	183	0.277	6.66
Cleaved E6						
340 g/L	—	—	0.287	37.2	0.287	—
480 g/L	—	—	0.290	57.1	0.290	—
620 g/L	—	—	0.291	108	0.291	—
760 g/L	**—**	**—**	**0.294**	**172**	**0.294**	**—**

Table S10: Fitting parameters of time-resolved anisotropy of representative intact and cleaved E6 probe in Ficoll-70 solutions. The angle (θ) between the absorbing and emitting dipoles is also calculated using the initial anisotropy. These were measured using the TCSPC technique with emission-polarization analysis of the acceptor.

$\lambda_x - \lambda_{fl}$:	β_1	φ_1	β_2	φ_2	r_0	θ	R_{DA}
425 – 531/40:		**(ns)**		**(ns)**			**(nm)**
E6							
100 g/L	0.078	1.57	0.159	26.5	0.238	48.8º	6.40
200 g/L	0.085	1.51	0.144	49.6	0.229	49.3º	6.18
300 g/L	0.086	1.12	0.142	78.2	0.228	49.3º	5.97
Cleaved E6							
100 g/L	—	—	0.278	21.9	0.278	46.7º	—
200 g/L	—	—	0.278	37.4	0.278	46.7º	—
300 g/L	—	—	**0.276**	**48.6**	**0.276**	**46.8º**	—